Published in final edited form as:
Aging Cell. 2009 April ; 8(2): 178–191. doi:10.1111/j.1474-9726.2009.00460.x.

The molecular architecture of myelinated peripheral nerves is supported by calorie restriction with aging

Sunitha Rangaraju[1], **David Hankins**[1], **Irina Madorsky**[1], **Evgenia Madorsky**[1], **Wei-Hua Lee**[1], **Christy S. Carter**[2], **Christiaan Leeuwenburgh**[2], and **Lucia Notterpek**[1]

[1]Dept. of Neuroscience, College of Medicine, McKnight Brain Institute, and The Institute on Aging, University of Florida, Gainesville, FL, USA

[2]Dept. of Aging and Geriatrics, College of Medicine, McKnight Brain Institute, and The Institute on Aging, University of Florida, Gainesville, FL, USA

Summary

Peripheral nerves from aged animals exhibit features of degeneration, including marked fiber loss, morphological irregularities in myelinated axons and notable reduction in the expression of myelin proteins. To investigate how protein homeostatic mechanisms change with age within the peripheral nervous system, we isolated Schwann cells from the sciatic nerves of young and old rats. The responsiveness of cells from aged nerves to stress stimuli is weakened, which in part may account for the observed age-associated alterations in glial and axonal proteins *in vivo*. While calorie restriction (CR) is known to slow the aging process in the central nervous system, its influence on peripheral nerves has not been investigated in detail. To determine if dietary restriction is beneficial for peripheral nerve health and glial function, we studied sciatic nerves from rats of four distinct ages (8-, 18-, 29- and 38-months) kept on an ad libitum (AL) or a 40% CR diet. Age-associated reduction in the expression of the major myelin proteins and widening of the nodes of Ranvier are attenuated by the dietary intervention, which is paralleled with the maintenance of a differentiated Schwann cell phenotype. The improvements in nerve architecture with diet restriction, in part, are underlined by sustained expression of protein chaperones and markers of the autophagy-lysosomal pathway. Together, the in vitro and in vivo results suggest that there might be an age-limit by which dietary intervention needs to be initiated to elicit a beneficial response on peripheral nerve health.

Keywords

peripheral nerve; Schwann cell; heat shock protein; autophagy; myelin; chaperones

Introduction

Aging is associated with structural, functional and biochemical alterations in the nervous system. Neurons with long processes are particularly vulnerable to degeneration (Mattson and Magnus, 2006), which makes peripheral nerves susceptible to age-related modifications. Signal propagation along axons is facilitated by myelin, a lipid-rich membranous structure formed by Schwann cells. Distinct domains within the myelin and the axonal plasma membrane are maintained by complex signaling events between neurons and glia (Garbay et al., 2000). Therefore, degenerative changes in either cell type have global influences on

Corresponding author: Lucia Notterpek, Ph.D., Dept. of Neuroscience, McKnight Brain Institute, 100 Newell Drive, Box 100244, Gainesville, FL 32610-0244, Phone: 352-294-0030; Fax: 352-846-3854; Email: notterp@mbi.ufl.edu .

overall nerve structure and function. Myelinated peripheral nerves from aged animals show fiber loss and morphological irregularities (Verdu et al., 2000), as well as a notable reduction in the expression of myelin and neurofilament genes and proteins (Parhad et al., 1995; Melcangi et al., 1998a; Melcangi et al., 1998b; Melcangi et al., 2000; Uchida et al., 2004). There is evidence for axonal demyelination and occasional remyelination in aged rat sciatic nerves, associated with nerve fiber degeneration (Sharma et al., 1980; Grover-Johnson and Spencer, 1981; Adinolfi et al., 1991). In response to demyelination, Schwann cells increase in number (Gregson and Hall, 1973) and dedifferentiate (Zanazzi et al., 2001). Age-associated functional changes include decline in nerve conduction velocity and muscle strength, and decreases in sensory discrimination, autonomic responses and endoneurial blood flow (Verdu et al., 2000). Together, these alterations contribute to decline in neuromuscular function and impact physical performance.

Reduction in the expression of functional proteins and the accumulation of damaged and misfolded proteins have been observed in a variety of organisms with age (Sitte et al., 2000; Squier, 2001; Calabrese et al., 2004; Keller et al., 2004; Grune et al., 2005). The extent to which damaged proteins accumulate is highly dependent upon the cell's capacity to repair or remove them by subcellular homeostatic mechanisms (Stadtman, 2001), namely chaperones and protein degradation. Chaperones (also referred to as heat shock proteins, HSPs) transiently interact with proteins to aid their folding, trafficking and degradation (Frydman, 2001; Sherman and Goldberg, 2001). Cellular degradative pathways include the ubiquitin-proteasome system (UPS) and the autophagy-lysosomal pathway (also referred to as autophagy). With an age-related decline in the activity of these homeostatic mechanisms, damaged proteins and organelles can accumulate and lead to cellular dysfunction and cell death (Macario and Conway de Macario, 2002; Bergamini et al., 2004). Metabolically active and postmitotic cells (Boulton et al., 2004; Weissman et al., 2007) such as neurons and myelinating Schwann cells are particularly sensitive to the accumulation of damaged proteins.

One approach to slow the aging process and prolong lifespan is through dietary modulation, such as calorie restriction (CR) (Johnson et al., 2006). Dietary restriction can induce HSPs (Heydari et al., 1996; Selsby et al., 2005) and autophagy (Bergamini et al., 2003; Wohlgemuth et al., 2007) and therefore support the maintenance of healthy cells and organs. While much work concerning dietary modulation has focused on the central nervous system (CNS), peripheral organs and lifespan (Feuers et al., 1989; Mattson et al., 2001; Jolly, 2004), little is known about the effects of such approach on peripheral nerves. In the CNS, life-long reduction in calorie intake has been shown to preserve long-term potentiation (Hori et al., 1992) and ameliorate age-related cognitive decline (Pitsikas and Algeri, 1992). In the periphery, the decline in muscle mass and strength with age is ameliorated with a life-long CR diet (Marzetti et al., 2008; Xu et al., 2008), which in part might be underlined by improved neural function.

Here we examine the chaperone and autophagic responses of Schwann cells isolated from young and aged nerves, and relate the findings to age-related biochemical and cellular alterations in peripheral nerves. Our results indicate that a life-long CR regimen supports the maintenance of the molecular architecture of myelinated axons, including the expression of essential axonal and glial proteins.

Results

Chaperone response of Schwann cells isolated from nerves of aged rats

We isolated Schwann cells from postnatal day 2 (P2) and aged (25-mo) rats to investigate the subcellular mechanisms underlying the age-related alterations in the molecular

architecture of myelinated peripheral nerves (Verdu et al., 2006). Schwann cells from young (P2–6) animals respond to *in vitro* manipulation of protein degradative and chaperone pathways and allow for mechanistic studies (Fortun et al., 2003; Fortun et al., 2007). We examined the chaperone response of the cells to starvation (Stv) and heat shock (HS) stimuli (Fig. 1A). Under control culture conditions (Ct), both cell populations express similar levels of HSP90, HSP70 and HSP40. Incubation of the cells in Stv medium is associated with a notable increase in HSP70 (Plakidou-Dymock and McGivan, 1994), particularly in young cells. Similarly, stimulation of HSPs by incubating the cells at 45 °C for 20 min (Cristofalo et al., 2004; Fortun et al., 2007) leads to a pronounced increase in the expression of HSP70 and a slight increase in HSP90 and HSP40 (Fig. 1A). Quantifications from three independent experiments indicate a nearly 5-fold greater HSP70 induction in P2 cells, as compared to cells from 25-mo old rats (*$p<0.05$). GAPDH levels are similar among the cells and paradigms tested.

To further investigate the muted chaperone response of the aged cells, we performed immunostaining with anti-HSP70 antibodies (Fig. 1B). As suggested by the biochemical data (Fig. 1A), Schwann cells cultured from P2 nerves show a robust induction of HSP70 (Fig. 1B, green), which is nearly uniform among all the cells. The low level of HSP70-like immunoreactivity in control cells is shown in the inset. In comparison, cells isolated from the 25-mo old rats exhibit notable heterogeneity in their ability to respond to HS, with only a fraction of the cells showing elevated HSP70 expression (Fig. 1B, green). Quantification of three independent experiments indicates that 42.48±6.14 % of 25-mo cells respond to HS in comparison to over 90.45±2.47 % of young (P2) cells (mean ± SEM; ***$p<0.001$). Therefore, the reduced level of HSP70 on the Western blots (Fig. 1A) is a reflection of the inability of a fraction of aged cells to respond to stress stimuli.

The autophagic response of glial cells is altered with age

Next, we tested Schwann cells isolated from P2 and 25-mo old rats for their autophagic capacity (Fig. 2). To stimulate autophagy, the cells were incubated in medium deprived of amino acids and serum (Stv medium) (Fortun et al., 2003) for 4 h followed by lysis. In a subset of samples, we simultaneously added chloroquine (CQ; 50 μM) to evaluate differences in the autophagic flux under conditions that inhibit lysosomal enzyme activity (Mizushima and Yoshimori, 2007). CQ is a lysosomotropic alkaline that increases the pH within lysosomes thereby inhibiting their proteolytic activity (Rocca et al., 2001). As a biochemical measure of autophagy, we evaluated the levels of Atg7 and lipidation of LC3 (Fig. 2A). The young (P2) cells respond to nutrient deprivation (Stv) by activating the autophagic pathway, as revealed by an increase in Atg7 and the conversion of LC3 I to LC3 II (lipidated form) (Kabeya et al., 2000;Mizushima and Yoshimori, 2007). In the old cells, the response to Stv is lessened, which is particularly notable for Atg7. Upon co-treatment with Stv medium and CQ, the levels of LC3 II further increase, indicating ongoing autophagic flux (Mizushima and Yoshimori, 2007;Klionsky et al., 2008). This trend is significantly (*$p<0.05$) more robust in cells from young, as compared to those from aged rats (Fig. 2B). Furthermore, in young cells (P2), the phosphorylated form of ribosomal protein S6 (pS6) disappears completely upon Stv (Blommaart et al., 1995), whereas in 25-mo old cells it does not (Fig. 2A). As expected, compared to Stv alone, the levels of pS6 slightly increase in the Stv+CQ co-treatment paradigm in both samples, confirming the specificity of this marker for the Stv-induced autophagy. Both young and old cells respond to Stv as seen by significant decline in the ratio of pS6 and S6 (Fig. 2C), a value that is used as a marker of autophagic activity (Blommaart et al., 1995). However, the ratio in 25-mo old samples is significantly higher (**$p<0.01$) than in P2 cells, indicating defective autophagy (Fig. 2C).

We also examined the expression of lysosomal proteins within the same samples and detected a slowed mobility of LAMP1 in aged cells (Fig. 2D, asterisk) To obtain insight into lysosomal proteolytic potential (Fusek and Vetvicka, 2005), we studied the expression of cathepsin D (cath D). The levels of pro-cathepsin D (pro-cath D) and active cath D under control conditions are lower in 25-mo cells as compared to P2 (Fig. 2D, 2E). There is a decrease in the active cath D upon CQ treatment in both ages, as this lysosomotropic agent increases the secretion of pro-cath D and prevents the processing of the active cath D (Samarel et al., 1989). Under Stv conditions, the active form of cath D is notably higher in young, as compared to 25-mo cells (Fig. 2E, $^{**}p<0.01$). This active form is depleted when Stv is combined with CQ treatment, thereby confirming the specificity of the Stv response in processing cath D. These results are consistent among three independent experiments (Fig. 2E) and suggest alterations in the autophagy-lysosomal activity of Schwann cells isolated from nerves of aged rats.

To examine the fusion of autophagic vacuoles with lysosomes, we double immunostained Schwann cells with LC3 and LAMP1 antibodies (Fig. 3). Schwann cells from P2 rats contain small LAMP1-positive lysosomes and relatively few LC3- reactive autophagosomes dispersed within the cytosol (Fig. 3A, panel on left, Ct). Subjecting the young cells to Stv increases the size of lysosomes (Fig. 3A, Stv, arrow) and the number of autophagosomes. On the other hand, Schwann cells from 25-mo rats show visibly large lysosomes under control conditions (Fig. 3A, panel on right, Ct, arrows) and only a modest increase in LAMP1-positive lysosomes upon Stv. In agreement with the biochemical results (Fig. 2A), the abundance of LC3-positive autophagosomes remains low in Stv-treated 25-mo Schwann cells (insets on right). To evaluate the autophagic flux, we analyzed the Stv+CQ treated cells by confocal microscopy (Fig. 3B). On representative single plane images, there are several fusion events of LC3-positive autophagosomes and LAMP1-positive lysosomes in Schwann cells from P2 rats (Fig. 3B, yellow spots). The fusion of lysosomes (green) with autophagosomes (red) is resolved in more detail on single plane sections (Fig. 3B, x and y sections). In agreement with the defective autophagosome-lysosome fusion hypothesis in old cells (Cuervo et al., 2005), there are fewer colocalization of LAMP1 and LC3 (yellow spots) within Schwann cells isolated from the old rats. 2D-cytofluorograms reveal more yellow pixels in young, as compared to old cells (Fig. 3C). Quantification of colocalization mask area shows a significant ($^{*}p<0.05$) reduction in autophagosome-lysosome fusion events in 25-mo cells (Fig. 3D). We completed a similar set of studies in cells isolated from the peripheral nerves of 5-mo old rats which behave similar to the P2 rats (data not shown). Together, these results indicate that Schwann cells isolated from aged nerves respond less vigorously to HS and Stv stimuli, as compared to neonatal (P2) or young-adult (5-mo) cells.

Protein homeostatic mechanisms are maintained in nerves of diet restricted rats

Protein homeostatic mechanisms that maintain tissue health and repair damage are known targets of age-related alterations (Rattan, 2004). To examine how age and diet affect the steady-state expression of protein chaperones within myelinated nerves, we focused on the HSP90/HSP70 network (Fig. 4A). Heat shock factor 1 (HSF1), a key regulator of this pathway, is held in an inactive state in the cytosol by HSP90. (Ohtsuka and Suzuki, 2000; Voellmy and Boellmann, 2007) and upon release it translocates to the nucleus, where it promotes the expression of HSP70, HSP27 and αB-crystallin (Pirkkala et al., 2001). The levels of HSF1 and HSP90 gradually increase with age in the AL group, a trend which is significant at 38-mo (Fig. 4A, 4B). The CR diet attenuates this pattern and is associated with sustained low level of HSF1. Upon analysis of the corresponding chaperones, we observe a significant increase in HSP90-like reactivity, while the steady-state levels of HSP70 and αB-crystallin appear to decline with age (Fig. 4A). Quantification of the data confirms the changes for HSP90 (Fig. 4B), but not for HSP70 and αB-crystallin (data not shown). The

steady-state expressions of HSP40 and of the small chaperone HSP27 are sustained across the studied samples.

Demyelination of nerves and accumulation of damaged proteins within Schwann cells elicits a proteolytic response, which is reflected by activation of the autophagy-lysosomal pathway (Notterpek et al., 1997; Fortun et al., 2003). In agreement with the known degenerative changes in peripheral nerves of aged rodents (Melcangi et al., 1998a; Verdu et al., 2000; Uchida et al., 2004), we found a gradual increase in the steady-state levels of LAMP1 and the autophagic protein Atg7 with age (Fig. 4C). The semi-quantitative analysis shows that this trend is lessened by the intervention, leading to balanced expression of both these proteins (Fig. 4C, 4D). Similarly, the age-associated increase in the levels of pS6 and total S6, are diminished by the intervention. The ratio of these two species (Blommaart et al., 1995) is significantly higher in the samples from the AL-fed 18-mo and 38-mo rats as compared to CR (Fig. 4E). However, the differences in the pS6/S6 ratios between AL and CR samples at 8- and 29-mo ages are not significant ($p=0.823$ and $p=0.526$, respectively). Overall, these data suggest that the degenerative changes are muted with CR, which decreases the demand on protein homeostatic mechanisms, including the autophagy-lysosomal pathway.

The expression of myelinated Schwann cell proteins in diet restricted rats

Efficient functioning of peripheral nerves is supported by myelin-forming Schwann cells. To examine the influence of the dietary restriction on peripheral nerve health, we prepared tissue lysates from sciatic nerves and studied the expression of glial and axonal proteins by Western blots (Fig. 5). Our results confirm earlier findings (Melcangi et al., 1998a;Melcangi et al., 2000) in a wide age group, where we detect gradual decline in three structural myelin proteins, including protein zero (P0), peripheral myelin protein 22 (PMP22) and myelin basic protein (MBP) (Fig. 5A). The decreases are pronounced by 29-mo of age, and reach statistical significance for all three proteins at 38-mo (Fig. 5B). In comparison, in nerve lysates from diet restricted animals, the levels of these proteins are maintained (Fig. 5A, 5B). We previously reported that rats kept on the CR diet display significantly better functional performance in the grip strength task (Ingram et al., 2007;Xu et al., 2008). Within the AL-fed group, there is a positive correlation between the decline in fore-limb grip strength and MBP expression ($p<0.001$), and an emerging trend for strength and PMP22 ($p=0.096$). Neither association is present in the CR-fed group ($p>0.05$). These data suggest that age-related loss of myelin is correlated with a decline in strength, and interventions such as CR, which slow myelin loss, may also preserve functional performance (Ingram et al., 2007;Xu et al., 2008).

In response to demyelination Schwann cells re-enter the cell cycle and proliferate (Jessen and Mirsky, 2005). Change in the differentiation state of Schwann cells is reflected by the re-expression of the p75 neurotrophin receptor ($p75^{NTR}$) (Jessen and Mirsky, 2005). In agreement, immunoblotting the nerve lysates with an anti-$p75^{NTR}$ antibody shows higher levels of this protein in the samples from 38-mo old AL-fed rats (Fig. 5C, 5D), as compared to the younger ages. This increase in expression is attenuated by the CR regimen, supporting the maintenance of the differentiated Schwann cell phenotype (Fig. 5D). In accordance, the levels of the mitotic marker, phosphorylated histone-3 (pHH3) (Ribalta et al., 2004) are higher in the AL-group as compared to CR (Fig. 5C, 5D). We also labeled nerve sections with Hoechst dye and counted the number of supernumerary Schwann cell nuclei, excluding epineurial and endoneurial cells (Fig. 5E). The average number of nuclei within fixed tissue area of 18-mo old AL-fed rats is 42.80 ± 0.98 ($n=3$, mean ± SEM) whereas there is a small but statistically significant decrease in response to the intervention (39.88 ± 1.24 nuclei, $^*p<0.05$). Significantly, there is a nearly 3-fold increase in the number of nuclei in the oldest samples (117.9 ± 6.08 vs. 42.80 ± 0.98), which is remarkably alleviated by CR (Fig. 5E).

Together, these results indicate that a life-long dietary restriction supports the maintenance of the differentiated Schwann cell phenotype, which is beneficial for myelin and axonal structure.

Axonal constituents in myelinated peripheral nerves of diet restricted rats

Schwann cells provide support for the functional integrity of myelinated axons (Nave and Trapp, 2008). Therefore, under conditions of myelin loss as seen in the aged nerves (Fig. 5A) alterations in axonal and structural proteins are expected. We corroborated the biochemical analysis of myelin proteins (Fig. 5) by double immunolabeling longitudinal nerve sections from 18- and 38-mo old rats with anti-MBP and neurofilament light chain (NF-L) protein antibodies (Fig. 6A). In agreement with the pronounced reduction in MBP in the nerve lysates (Fig. 5A) in samples from AL 38-mo old animals there are NF-L antibody-reactive axons devoid of myelin (Fig. 6A, arrowheads). In contrast, nerves of 38-mo old CR rat show a remarkable maintenance of MBP-positive internodes (Fig. 6A, red) and only few axons without myelin (arrowheads). Immunostaining for NF-heavy (NF-H) and -medium (NF-M) chain protein shows similar pattern (data not shown). Nerve sections from 18-mo old rats are included for comparison (Fig. 6A, insets in top panels).

Since there seem to be fewer NF-reactive fibers in AL-fed 38-mo old samples (Fig. 6A), we analyzed the levels of the three major NF proteins (Fig. 6B). In agreement with previous reports (Parhad et al., 1995;Uchida and Brown, 2004;Uchida et al., 2004), nerves from 38-mo old rodents show reduction in the steady-state expression of NF-H, -M and -L (trend for NF-H and significant for NF-M and NF-L) (Fig. 6B, 6C). Strikingly, their levels are maintained in rats on the intervention (Fig. 6C), corresponding to the immunolabeling studies (Fig. 6A). In sciatic nerve samples from our oldest AL-fed rats, vimentin, an intermediate filament protein expressed by Schwann cells and neurons (Toth et al., 2008), appears to undergo proteolytic degradation (Fig. 6B, square bracket). This aberrant phenotype, which may be a reflection of enhanced caspase activity in aged nerves (Byun et al., 2001), is absent from independent samples on the dietary regimen (Fig. 6B). Together these results show that the CR intervention supports maintained expression of glial and axonal gene products, including myelin and neurofilament proteins.

Demyelination of nerve fibers with age and disease leads to spreading of voltage-gated ion channels in the axonal membrane (Adinolfi et al., 1991; Verdu et al., 2000; Amici et al., 2007). To determine if the CR diet supports the expression of channel proteins at nodes of Ranvier, we performed biochemical and immunohistochemical analyses of pan-voltage gated sodium channels (Na_v) and voltage gated potassium channels (Kv1.1) (Fig. 7). While the steady-state levels of both Na_v and Kv1.1 dramatically increase with age in the AL-fed group, especially at 38-mo (6-fold increase for Na_v and 7-fold increase for Kv1.1), in nerves from CR animals such changes are muted (*$p<0.05$ for both Na_v and Kv1.1) (Fig. 7A). Furthermore, proteolytic cleavage of the α-subunit of Na_v channels (Zwerling et al., 1991; Benz et al., 1997), most notable in the 38-mo sample (Fig. 7A, arrowhead), is lessened by the intervention.

We confirmed the biochemical results by co-immunolabeling nerve sections with antibodies against Na_v or Kv1.1 channels, and MBP (Fig. 7B, C). As suggested by the higher expression level of the channel proteins (Fig. 7A) and the abundance of unmyelinated fibers (Fig. 6A), Na_v channel-like immunoreactivity is prominent and diffuse along unmyelinated axons in nerves from 38-mo old AL-fed rats (Fig. 7B). Furthermore, there is wider distribution of Na_v at nodes of Ranvier (Fig. 7B, asterisks and insets in top panel), likely due to segmental demyelination. In comparison, focal localization of Na_v channel is maintained in samples from 38-mo old rodents on the regimen (Fig. 7B, asterisks and insets in bottom panel). Similarly, the Kv1.1 channel-like immunoreactivity is spread along axons in nerve

sections from 38-mo AL rats (Fig. 7C), instead of being confined to the paranodal region. Again, in response to dietary restriction, spatial localization of Kv1.1 is maintained to the paranodal region (Fig. 7C). Together, these results show a beneficial effect of CR on the molecular architecture of myelinated peripheral nerves, including the expression and localization of glial and axonal proteins (Fig. 5–Fig. 7).

Discussion

Glial cells isolated from aged rats have muted response to stress stimuli, which may in part underlie the degenerative changes observed with age in myelinated peripheral nerves. Reduction in calorie intake, the most widely accepted and effective method of defying age-related alterations (Everitt et al., 2006), preserves the molecular architecture of myelinated axons likely by supporting Schwann cell function. The benefits are evident by maintained expression and correct localization of glial and axonal molecules, including myelin, neurofilament and ion channel proteins. Constituents of protein homeostatic mechanisms remain leveled in nerves from diet restricted rats, potentially reflecting lower demand on these pathways.

While CR diet affects specific physiologic parameters and cellular pathways in different organs (Mattson et al., 2001), here we focused on two protein homeostatic mechanisms, namely chaperones and autophagy. We isolated Schwann cells from myelinated nerves of young and old rats and found notable differences in their chaperone responses (Fig. 1). The muted response of old glial cells at least in part is reminiscent of the findings from the nerves of AL-fed aged animals (Fig. 4). In sciatic nerve lysates, we detected a prominent increase in the steady-state expression of HSF1 at 38-mo (Fig. 4), which may indicate a compensatory attempt for compromised signaling of the HSP90/HSF1 pathway (Ohtsuka and Suzuki, 2000; Voellmy and Boellmann, 2007). In agreement, while there is an increase in HSP90-like reactivity, the steady-state levels of HSP70 and αB-crystallin are low. Age-related increase in HSF1 levels have been previously reported in isolated rat hepatocytes and is associated with a decline in binding activity of HSF1 with heat shock elements (Heydari et al., 2000). A crucial role for chaperones in myelinated nerves is supported by the ATP-dependent interaction of HSP70 with MBP (Lund et al., 2006). Constitutive expression of HSC70 appears to be also necessary for the correct expression of MBP during the differentiation of oligodendrocytes (Aquino et al., 1996), suggesting HSP70 is involved in the proper folding and trafficking of this myelin protein. Furthermore, *hsf1* knock-out mice exhibit a demyelinating phenotype in the CNS, likely due to defective oligodendrocyte differentiation, or myelin synthesis and assembly (Homma et al., 2007). Complimentarily, the enhancement of HSPs improves myelination in a neuropathic model (Rangaraju et al., 2008). Thus, the decline in the ability of Schwann cells to induce chaperones may impair their ability to sustain and repair myelin with age. CR diet has the ability to prevent the aforementioned decrease in HSF1 binding activity (Heydari et al., 1996), and support the expression of chaperones.

In aged cells, macroautophagy is known to be defective both in the formation and clearance of autophagosomes (Cuervo et al., 2005). Poor elimination of autophagosomes could result from a decrease in lysosomal enzyme activity and/or impaired fusion of lysosomes with autophagosomes (Cuervo et al., 2005). Our data support these hypotheses, as Schwann cells from old rats show low levels of the lysosomal endoprotease, cath D with Stv, and prominent swollen lysosomes and few fusion events of autophagosomes and lysosomes (Fig. 2 and Fig. 3). Although the overall levels of LAMP1 are unchanged by the modulation, the mobility of LAMP1 is slowed in old cells, possibly due to altered glycosylation, or compromised pathway activity. Indeed, Schwann cells isolated from old rats contain visibly larger lysosomes under basal conditions (Fig. 3A), as compared to young cells. In addition,

the described alterations in biochemical markers of the autophagy-lysosome pathway (Atg7, LC3 and pS6/S6 ratios) suggest that autophagy becomes less efficient with age. It has been previously shown that phosphorylation of S6 and inhibition of autophagy have a linear relationship in rat hepatocytes (Blommaart et al., 1995). In our model, based upon the levels of pS6 in response to Stv the activation of autophagy is minimal in Schwann cells from 25-mo old rats (Fig. 2A). The maintenance of autophagy with diet restriction in sciatic nerves is likely mediated via S6 kinase (Klionsky et al., 2005), which is reflected upon the lower levels of pS6 in 38-mo CR rat nerves as compared to AL.

Peripheral nerves serve as long cables connecting the CNS with distal targets, such as skeletal muscle. The function of peripheral nerves is affected by age and is associated with morphologic (Verdu et al., 2000) and biochemical myelin abnormalities (Fig. 5–Fig. 6). Defective myelin and segmental demyelination are coupled with dedifferentiation of Schwann cells (Gregson and Hall, 1973; Saito et al., 1990; Zanazzi et al., 2001). We observed this switch in phenotype in the aged nerves from AL-fed rats by re-expression of $p75^{NTR}$ (Fig. 5C), which is detected only at low levels when the cells are in a myelinating state (Jessen and Mirsky, 2005; Amici et al., 2007). In nerves from rats on the diet-regimen, myelin maintenance is associated with subdued expression of $p75^{NTR}$ and the mitotic marker, pHH3 (Fig. 5). Prevention of demyelination and hyperproliferation of Schwann cells with age suggest better axo-glial communication in diet restricted animals, which supports the maintenance of the major structural proteins of axons. Together, the prevention of glial and axonal changes preserves the functional architecture of myelinated nerves (Fig. 5–Fig. 7) and is associated with improved motor performance (Xu et al., 2008).

Demyelination of axons leads to a decrease in nerve conduction velocity and reorganization of voltage-sensitive ion channels has been suggested as an underlying cause (Adinolfi et al., 1991; Verdu et al., 2000). The cross-talk between axons and glia is responsible for maintaining the proper localization of ion channels (Novakovic et al., 2001; Hinman et al., 2006). In this study, we found segmental demyelination in nerves from AL-fed aged rats and a corresponding redistribution of ion channels (Fig. 7). In transgenic mice, when Schwann cells are selectively killed by diphtheria toxin, a demyelinating phenotype is associated with overexpression and redistribution of sodium channels (Vabnick et al., 1997). Similarly, a knock-out mouse with deletion of MBP shows a strikingly high density of Na channels along hypomyelinated axons (Noebels et al., 1991; Westenbroek et al., 1992), likely as a compensatory mechanism to support signal propagation. Nonetheless, the redistribution in ion channel proteins associated with defective myelination is not an effective replacement of myelinated internodes and can lead to sensory and motor dysfunction (Novakovic et al., 2001). Our study shows that the CR regimen has the ability to minimize the changes in expression and organization of the Na_v and Kv channel at the node of Ranvier (Fig. 7), likely by preservation of internodal myelin segments.

Together, the muted responsiveness of stress induced pathways in aged Schwann cells might exacerbate the observed molecular and structural defects in myelinated peripheral nerves. Approaches to limit the demand on protein homeostatic pathways, such as dietary restriction appear to provide benefits for maintenance of nerve health.

Experimental Procedures

Animals and diets

To establish rat Schwann cell cultures, we used male Fischer 344 rats from National Institute on Aging colony at Harlan Sprague Dawley Inc (Indianapolis, IA) (Norris et al., 1996). For dietary modulation studies, Male Fisher 344 × BN (Brown Norway) rats of four distinct ages 8-, 18-, 29- and 38-months (mo) and specified diets were obtained from the National

Institute on Aging colony. Ad libitum (AL) fed rats had free access to NIH-31 average nutrient composition pellets, whereas the calorie restricted (CR) group received fortified pellets once daily, 1 h before the onset of the dark period. The dietary restriction was initiated at 14 weeks of age with 10 % restriction, increased to 25% at 15 weeks, and continued at 40% from 16 weeks of age. Both the AL and CR rats had access to water at all times. The use of animals in this study was approved by an Institutional Animal Care and Use Committee of the University of Florida.

Primary culture of Schwann cells from young and old rats

Schwann cell cultures were established from the sciatic nerves of postnatal day 2 (P2) 5-mo and 25-mo old rats using established procedures (Notterpek et al., 1999). Nerves were dissected and gently stripped of connective tissue and epineurium, chopped into small pieces and digested over a period of 1 h for P2 (young) and 5 h for the adult samples, at 37 °C in a humidified atmosphere of 5 % CO_2. The digestion medium consisted of Dulbecco's Modification of Eagle's Medium (DMEM) (Gibco, Grand Island, NY), 15 % Fetal Bovine Serum (FBS) (Hyclone, Logan, UT), penicillin streptomycin (Gibco) and an enzyme cocktail of 0.03 % collagenase type III (Worthington, Lakewood, NJ), 0.1 % hyaluronidase (Sigma-Aldrich), 1.25 units/mL dispase (Worthington). Following digestion, cell suspensions were washed once and resuspended in culture medium (DMEM containing 10 % FBS). Cells were then plated in small drops on poly-L-lysine (Sigma-Aldrich) coated glass cover slips or on plastic petri-dishes and allowed to adhere overnight. The next day, cells were washed with DMEM followed by addition of DMEM containing 10 % FBS, 10 μM of antimitotic agent cytosine β-D-arabinofuranoside (Sigma-Aldrich), to eradicate contaminating fibroblasts. After four 24 h periods of antimitotic treatments, given on alternate days, standard growth medium (DMEM containing 10 % FBS, 10 μg/mL bovine pituitary extract [Biomedical Technologies, Inc., Stroughton, MA] and 5 μM forskolin [Calbiochem, La Jolla, CA]) was added and the cells were allowed to proliferate for 7–8 days. For the heat shock (HS) treatments, the cells were incubated at 45 °C for 20 min, followed by a recovery for 6 h (Cristofalo et al., 2004). Starvation (Stv) medium (amino acid- and serum-free) was used to stimulate autophagy (Fortun et al., 2003; Fortun et al., 2007). To estimate the autophagic flux, chloroquine (CQ; 50 μM) was added simultaneously with Stv condition for 4 h. After the specified treatments, samples were processed for biochemical or immunochemical studies.

Biochemical studies

Sciatic nerves isolated from AL and CR rats (n=3) were frozen immediately and stored in liquid nitrogen. Cultured Schwann cells were washed twice with ice cold PBS followed by lysis. Cell or nerve lysates were prepared in sodium dodecyl sulfate (SDS) sample buffer (62.5 mM Tris, pH 6.8, 10 % glycerol, 3 % SDS) supplemented with phosphatase inhibitors, PMSF (both from Sigma-Aldrich, St. Louis, MO) and complete protease inhibitor (Roche, Indianapolis, IN). Protein concentrations were determined using the BCA protein assay kit (Pierce Chemicals, Rockford, IL). Protein samples (5–25 μg/lane) were separated on 7.5 %, 10 %, 12.5 % or 15 % SDS-polyacrylamide gels under reducing conditions and proteins were transferred to nitrocellulose or Polyvinylidene Flouride (PVDF) membranes (for LC3) (both from Bio-Rad Laboratories, Hercules, CA). Membranes were blocked in 5 % non-fat milk in PBS and incubated overnight with primary antibodies (See Table 1). After washing, anti-mouse, anti-rabbit (both from Cell Signaling Technology), anti-chicken or anti-rat (both from Sigma-Aldrich) HRP-linked secondary antibodies were added for 2 h. Bound antibodies were visualized using an enhanced chemiluminescence detection kit (PerkinElmer Life Sciences, Boston, MA). Films were digitally imaged using a GS-710 densitometer (Bio-Rad Laboratories) and were formatted for printing by using Adobe Photoshop 5.5. Semi-quantitative analysis of protein levels was performed using Scion

image software. The relative densitometric units were determined after normalizing with a protein loading control. For the nerves, the value of 8-mo old AL sample was set to 1 and the values of other age-diet combination were determined with respect to this. One way ANOVA followed by Fisher's PLSD analysis was performed using the StatView program, to compare the normalized densitometric values of proteins (dependent variables) between AL and CR diet with age (factor). To determine statistical significance between samples, unpaired t-test was performed using GraphPad Prism v5.0 software.Graph pad Prism software.

Immunochemistry

Schwann cells on glass coverslips were fixed with 4 % paraformaldehyde (10 min) and permeabilized with ice-cold 100% methanol (5 min). Sciatic nerves from rats were dissected and frozen by immersion in liquid nitrogen. Frozen nerves were longitudinally sectioned (5 μm thickness) using Leica CM1850 cryostat and were dried on Superfrost/Plus microslides (Fisher, Pittsburgh, PA) for 1 h. Dried tissue sections were fixed with 4 % paraformaldehyde for 1 h, permeabilized with ice-cold 100 % methanol (5 min) or acetone (2 min) and processed for immunostaining (Ryan et al., 2002). After an overnight incubation at 4 °C, bound antibodies (see Table 1) were detected using Alexa Fluor 594-conjugated (red) anti-rabbit and Alexa Fluor 488-conjugated (green) anti-mouse secondary antibodies (Molecular Probes, Eugene, OR). To visualize the nuclei, Hoechst dye (Molecular Probes) was included with the secondary antibodies. Control samples without primary antibodies were processed in parallel. Cover slips were mounted using the Prolong Antifade kit (Molecular Probes). Images were acquired with a SPOT digital camera attached to a Nikon Eclipse 800 microscope Leica TCS SP2 confocal laser scanning microscope and processed for printing by using Adobe Photoshop 5.5.

Colocalization of LC3 and LAMP1

For analysis of colocalization of LC3 and LAMP1, images were acquired on a 63× water immersion lens using the Leica confocal microscope and z-stack images were captured. The 2D cytofluorograms in Figure 3C were created using Leica software with the same exposure settings for red and green channels for P2 and 25-mo samples. The software quantifies the extent of colocalization by creation of a binary mask for all of the pixels that are double positive for both LC3 and LAMP1 fluorescence so that colocalizing elements will appear in the diagonal of the cytofluorogram (Fig. 3C, outlined in green). Colocalization of LC3 and LAMP1 was then quantified by comparing the colocalization mask areas (in μm^2), normalized per cell, between P2 and 25-mo samples treated with Stv+CQ from three independent experiments (n=8 random visual fields per condition). Statistical significance was determined by unpaired t-test using GraphPad Prism v5.0 software.

Nuclei count

The nuclei (stained with Hoechst) of non-epineurial and non-endoneurial cells were counted in longitudinal sections (5 μm thickness) of sciatic nerves from two different depths and eight random visual fields ($0.1mm^2$) per animal (n=3). Statistical significance was determined by unpaired t-test using GraphPad Prism v5.0 software.

Abbreviations

PNS	peripheral nervous system
CNS	central nervous system
CR	calorie restriction

AL	ad libitum
P2	postnatal day 2
mo	month
HS	heat shock
HSP	heat shock protein
HSF1	heat shock factor 1
Stv	starvation
CQ	chloroquine
Atg	autophagy related homolog
LAMP1	lysosome associated membrane protein 1
pS6	phosphorylated S6
P0	protein zero
PMP22	peripheral myelin protein 22
MBP	myelin basic protein
pHH3	phosphorylated histone 3
NF	neurofilament
Na_v	voltage gated sodium channel
Kv	voltage gated potassium channel
GAPDH	glyceraldehyde 3-phosphate dehydrogenase

Acknowledgments

The authors wish to thank Doug Smith for technical assistance with the confocal microscopy. These studies were supported in part by the National Muscular Dystrophy Association and US National Institutes of Health grants NS041012 to LN, 5R01AG021042-04 to CL and RO1-AG024526 to CC.

References

Adinolfi AM, Yamuy J, Morales FR, Chase MH. Segmental demyelination in peripheral nerves of old cats. Neurobiol Aging. 1991; 12:175–179. [PubMed: 2052131]

Amici SA, Dunn WA Jr, Notterpek L. Developmental abnormalities in the nerves of peripheral myelin protein 22-deficient mice. J Neurosci Res. 2007; 85:238–249. [PubMed: 17131416]

Aquino DA, Lopez C, Farooq M. Antisense oligonucleotide to the 70-kDa heat shock cognate protein inhibits synthesis of myelin basic protein. Neurochem Res. 1996; 21:417–422. [PubMed: 8734434]

Benz I, Beck W, Kraas W, Stoll D, Jung G, Kohlhardt M. Two types of modified cardiac Na+ channels after cytosolic interventions at the alpha-subunit capable of removing Na+ inactivation. Eur Biophys J. 1997; 25:189–200. [PubMed: 9037754]

Bergamini E, Cavallini G, Donati A, Gori Z. The anti-ageing effects of caloric restriction may involve stimulation of macroautophagy and lysosomal degradation, and can be intensified pharmacologically. Biomed Pharmacother. 2003; 57:203–208. [PubMed: 12888255]

Bergamini E, Cavallini G, Donati A, Gori Z. The role of macroautophagy in the ageing process, anti-ageing intervention and age-associated diseases. Int J Biochem Cell Biol. 2004; 36:2392–2404. [PubMed: 15325580]

Blommaart EF, Luiken JJ, Blommaart PJ, van Woerkom GM, Meijer AJ. Phosphorylation of ribosomal protein S6 is inhibitory for autophagy in isolated rat hepatocytes. J Biol Chem. 1995; 270:2320–2326. [PubMed: 7836465]

Boulton M, Rozanowska M, Rozanowski B, Wess T. The photoreactivity of ocular lipofuscin. Photochem Photobiol Sci. 2004; 3:759–764. [PubMed: 15295632]

Byun Y, Chen F, Chang R, Trivedi M, Green KJ, Cryns VL. Caspase cleavage of vimentin disrupts intermediate filaments and promotes apoptosis. Cell Death Differ. 2001; 8:443–450. [PubMed: 11423904]

Calabrese V, Scapagnini G, Ravagna A, Colombrita C, Spadaro F, Butterfield DA, Giuffrida Stella AM. Increased expression of heat shock proteins in rat brain during aging: relationship with mitochondrial function and glutathione redox state. Mech Ageing Dev. 2004; 125:325–335. [PubMed: 15063109]

Cristofalo VJ, Lorenzini A, Allen RG, Torres C, Tresini M. Replicative senescence: a critical review. Mech Ageing Dev. 2004; 125:827–848. [PubMed: 15541776]

Cuervo AM, Bergamini E, Brunk UT, Droge W, Ffrench M, Terman A. Autophagy and aging: the importance of maintaining “clean” cells. Autophagy. 2005; 1:131–140. [PubMed: 16874025]

Everitt AV, Hilmer SN, Brand-Miller JC, Jamieson HA, Truswell AS, Sharma AP, Mason RS, Morris BJ, Le Couteur DG. Dietary approaches that delay age-related diseases. Clin Interv Aging. 2006; 1:11–31. [PubMed: 18047254]

Feuers RJ, Duffy PH, Leakey JA, Turturro A, Mittelstaedt RA, Hart RW. Effect of chronic caloric restriction on hepatic enzymes of intermediary metabolism in the male Fischer 344 rat. Mech Ageing Dev. 1989; 48:179–189. [PubMed: 2661933]

Fortun J, Dunn WA Jr, Joy S, Li J, Notterpek L. Emerging role for autophagy in the removal of aggresomes in Schwann cells. J Neurosci. 2003; 23:10672–10680. [PubMed: 14627652]

Fortun J, Verrier JD, Go JC, Madorsky I, Dunn WA, Notterpek L. The formation of peripheral myelin protein 22 aggregates is hindered by the enhancement of autophagy and expression of cytoplasmic chaperones. Neurobiol Dis. 2007; 25:252–265. [PubMed: 17174099]

Frydman J. Folding of newly translated proteins in vivo: the role of molecular chaperones. Annu Rev Biochem. 2001; 70:603–647. [PubMed: 11395418]

Fusek M, Vetvicka V. Dual role of cathepsin D: ligand and protease. Biomed Pap Med Fac Univ Palacky Olomouc Czech Repub. 2005; 149:43–50. [PubMed: 16170387]

Garbay B, Heape AM, Sargueil F, Cassagne C. Myelin synthesis in the peripheral nervous system. Prog Neurobiol. 2000; 61:267–304. [PubMed: 10727776]

Gregson NA, Hall SM. A quantitative analysis of the effects of the intraneural injection of lysophosphatidyl choline. J Cell Sci. 1973; 13:257–277. [PubMed: 4729938]

Grover-Johnson N, Spencer PS. Peripheral nerve abnormalities in aging rats. J Neuropathol Exp Neurol. 1981; 40:155–165. [PubMed: 7463100]

Grune T, Merker K, Jung T, Sitte N, Davies KJ. Protein oxidation and degradation during postmitotic senescence. Free Radic Biol Med. 2005; 39:1208–1215. [PubMed: 16214036]

Heydari AR, You S, Takahashi R, Gutsmann A, Sarge KD, Richardson A. Effect of caloric restriction on the expression of heat shock protein 70 and the activation of heat shock transcription factor 1. Dev Genet. 1996; 18:114–124. [PubMed: 8934873]

Heydari AR, You S, Takahashi R, Gutsmann-Conrad A, Sarge KD, Richardson A. Age-related alterations in the activation of heat shock transcription factor 1 in rat hepatocytes. Exp Cell Res. 2000; 256:83–93. [PubMed: 10739655]

Hinman JD, Peters A, Cabral H, Rosene DL, Hollander W, Rasband MN, Abraham CR. Age-related molecular reorganization at the node of Ranvier. J Comp Neurol. 2006; 495:351–362. [PubMed: 16485288]

Homma S, Jin X, Wang G, Tu N, Min J, Yanasak N, Mivechi NF. Demyelination, astrogliosis, and accumulation of ubiquitinated proteins, hallmarks of CNS disease in hsf1-deficient mice. J Neurosci. 2007; 27:7974–7986. [PubMed: 17652588]

Hori N, Hirotsu I, Davis PJ, Carpenter DO. Long-term potentiation is lost in aged rats but preserved by calorie restriction. Neuroreport. 1992; 3:1085–1088. [PubMed: 1337284]

Ingram DK, Young J, Mattison JA. Calorie restriction in nonhuman primates: assessing effects on brain and behavioral aging. Neuroscience. 2007; 145:1359–1364. [PubMed: 17223278]

Jessen KR, Mirsky R. The origin and development of glial cells in peripheral nerves. Nat Rev Neurosci. 2005; 6:671–682. [PubMed: 16136171]

Johnson JB, Laub DR, John S. The effect on health of alternate day calorie restriction: eating less and more than needed on alternate days prolongs life. Med Hypotheses. 2006; 67:209–211. [PubMed: 16529878]

Jolly CA. Dietary restriction and immune function. J Nutr. 2004; 134:1853–1856. [PubMed: 15284365]

Kabeya Y, Mizushima N, Ueno T, Yamamoto A, Kirisako T, Noda T, Kominami E, Ohsumi Y, Yoshimori T. LC3, a mammalian homologue of yeast Apg8p, is localized in autophagosome membranes after processing. Embo J. 2000; 19:5720–5728. [PubMed: 11060023]

Keller JN, Dimayuga E, Chen Q, Thorpe J, Gee J, Ding Q. Autophagy, proteasomes, lipofuscin, and oxidative stress in the aging brain. Int J Biochem Cell Biol. 2004; 36:2376–2391. [PubMed: 15325579]

Klionsky DJ, Meijer AJ, Codogno P. Autophagy and p70S6 kinase. Autophagy. 2005; 1:59–60. discussion 60–51. [PubMed: 16874035]

Klionsky DJ, Abeliovich H, Agostinis P, Agrawal DK, Aliev G, Askew DS, Baba M, Baehrecke EH, Bahr BA, Ballabio A, Bamber BA, Bassham DC, Bergamini E, Bi X, Biard-Piechaczyk M, Blum JS, Bredesen DE, Brodsky JL, Brumell JH, Brunk UT, Bursch W, Camougrand N, Cebollero E, Cecconi F, Chen Y, Chin LS, Choi A, Chu CT, Chung J, Clarke PG, Clark RS, Clarke SG, Clave C, Cleveland JL, Codogno P, Colombo MI, Coto-Montes A, Cregg JM, Cuervo AM, Debnath J, Demarchi F, Dennis PB, Dennis PA, Deretic V, Devenish RJ, Di Sano F, Dice JF, Difiglia M, Dinesh-Kumar S, Distelhorst CW, Djavaheri-Mergny M, Dorsey FC, Droge W, Dron M, Dunn WA Jr, Duszenko M, Eissa NT, Elazar Z, Esclatine A, Eskelinen EL, Fesus L, Finley KD, Fuentes JM, Fueyo J, Fujisaki K, Galliot B, Gao FB, Gewirtz DA, Gibson SB, Gohla A, Goldberg AL, Gonzalez R, Gonzalez-Estevez C, Gorski S, Gottlieb RA, Haussinger D, He YW, Heidenreich K, Hill JA, Hoyer-Hansen M, Hu X, Huang WP, Iwasaki A, Jaattela M, Jackson WT, Jiang X, Jin S, Johansen T, Jung JU, Kadowaki M, Kang C, Kelekar A, Kessel DH, Kiel JA, Kim HP, Kimchi A, Kinsella TJ, Kiselyov K, Kitamoto K, Knecht E, et al. Guidelines for the use and interpretation of assays for monitoring autophagy in higher eukaryotes. Autophagy. 2008; 4:151–175. [PubMed: 18188003]

Lund BT, Chakryan Y, Ashikian N, Mnatsakanyan L, Bevan CJ, Aguilera R, Gallaher T, Jakowec MW. Association of MBP peptides with Hsp70 in normal appearing human white matter. J Neurol Sci. 2006; 249:122–134. [PubMed: 16842822]

Macario AJ, Conway de Macario E. Sick chaperones and ageing: a perspective. Ageing Res Rev. 2002; 1:295–311. [PubMed: 12039444]

Marzetti E, Lawler JM, Hiona A, Manini T, Seo AY, Leeuwenburgh C. Modulation of age-induced apoptotic signaling and cellular remodeling by exercise and calorie restriction in skeletal muscle. Free Radic Biol Med. 2008; 44:160–168. [PubMed: 18191752]

Mattson MP, Magnus T. Ageing and neuronal vulnerability. Nat Rev Neurosci. 2006; 7:278–294. [PubMed: 16552414]

Mattson MP, Duan W, Lee J, Guo Z. Suppression of brain aging and neurodegenerative disorders by dietary restriction and environmental enrichment: molecular mechanisms. Mech Ageing Dev. 2001; 122:757–778. [PubMed: 11322996]

Melcangi RC, Magnaghi V, Martini L. Aging in peripheral nerves: regulation of myelin protein genes by steroid hormones. Prog Neurobiol. 2000; 60:291–308. [PubMed: 10658644]

Melcangi RC, Magnaghi V, Cavarretta I, Martini L, Piva F. Age-induced decrease of glycoprotein Po and myelin basic protein gene expression in the rat sciatic nerve. Repair by steroid derivatives. Neuroscience. 1998a; 85:569–578. [PubMed: 9622253]

Melcangi RC, Magnaghi V, Cavarretta I, Riva MA, Piva F, Martini L. Effects of steroid hormones on gene expression of glial markers in the central and peripheral nervous system: variations induced by aging. Exp Gerontol. 1998b; 33:827–836. [PubMed: 9951626]

Mizushima N, Yoshimori T. How to interpret LC3 immunoblotting. Autophagy. 2007; 3:542–545. [PubMed: 17611390]

Nave KA, Trapp BD. Axon-glial signaling and the glial support of axon function. Annu Rev Neurosci. 2008; 31:535–561. [PubMed: 18558866]

Noebels JL, Marcom PK, Jalilian-Tehrani MH. Sodium channel density in hypomyelinated brain increased by myelin basic protein gene deletion. Nature. 1991; 352:431–434. [PubMed: 1713650]

Norris CM, Korol DL, Foster TC. Increased susceptibility to induction of long-term depression and long-term potentiation reversal during aging. J Neurosci. 1996; 16:5382–5392. [PubMed: 8757251]

Notterpek L, Shooter EM, Snipes GJ. Upregulation of the endosomal-lysosomal pathway in the trembler-J neuropathy. J Neurosci. 1997; 17:4190–4200. [PubMed: 9151736]

Notterpek L, Snipes GJ, Shooter EM. Temporal expression pattern of peripheral myelin protein 22 during in vivo and in vitro myelination. Glia. 1999; 25:358–369. [PubMed: 10028918]

Novakovic SD, Eglen RM, Hunter JC. Regulation of Na+ channel distribution in the nervous system. Trends Neurosci. 2001; 24:473–478. [PubMed: 11476887]

Ohtsuka K, Suzuki T. Roles of molecular chaperones in the nervous system. Brain Res Bull. 2000; 53:141–146. [PubMed: 11044589]

Parhad IM, Scott JN, Cellars LA, Bains JS, Krekoski CA, Clark AW. Axonal atrophy in aging is associated with a decline in neurofilament gene expression. J Neurosci Res. 1995; 41:355–366. [PubMed: 7563228]

Pirkkala L, Nykanen P, Sistonen L. Roles of the heat shock transcription factors in regulation of the heat shock response and beyond. Faseb J. 2001; 15:1118–1131. [PubMed: 11344080]

Pitsikas N, Algeri S. Deterioration of spatial and nonspatial reference and working memory in aged rats: protective effect of life-long calorie restriction. Neurobiol Aging. 1992; 13:369–373. [PubMed: 1625765]

Plakidou-Dymock S, McGivan JD. Amino acid deprivation-induced stress response in the bovine renal epithelial cell line NBL-1: induction of HSP 70 by phenylalanine. Biochim Biophys Acta. 1994; 1224:189–197. [PubMed: 7981232]

Rangaraju S, Madorsky I, Pileggi JG, Kamal A, Notterpek L. Pharmacological induction of the heat shock response improves myelination in a neuropathic model. Neurobiol Dis. 2008

Rattan SI. Hormetic mechanisms of anti-aging and rejuvenating effects of repeated mild heat stress on human fibroblasts in vitro. Rejuvenation Res. 2004; 7:40–48. [PubMed: 15256044]

Ribalta T, McCutcheon IE, Aldape KD, Bruner JM, Fuller GN. The mitosis-specific antibody anti-phosphohistone-H3 (PHH3) facilitates rapid reliable grading of meningiomas according to WHO 2000 criteria. Am J Surg Pathol. 2004; 28:1532–1536. [PubMed: 15489659]

Rocca A, Lamaze C, Subtil A, Dautry-Varsat A. Involvement of the ubiquitin/proteasome system in sorting of the interleukin 2 receptor beta chain to late endocytic compartments. Mol Biol Cell. 2001; 12:1293–1301. [PubMed: 11359922]

Ryan MC, Shooter EM, Notterpek L. Aggresome formation in neuropathy models based on peripheral myelin protein 22 mutations. Neurobiol Dis. 2002; 10:109–118. [PubMed: 12127149]

Saito H, Kobayashi K, Mochizuki H, Ishii T. Axonal degeneration of the peripheral nerves and postganglionic anhidrosis in a patient with multiple sclerosis. Tohoku J Exp Med. 1990; 162:279–291. [PubMed: 1965353]

Samarel AM, Ferguson AG, Decker RS, Lesch M. Effects of cysteine protease inhibitors on rabbit cathepsin D maturation. Am J Physiol. 1989; 257:C1069–C1079. [PubMed: 2610247]

Selsby JT, Judge AR, Yimlamai T, Leeuwenburgh C, Dodd SL. Life long calorie restriction increases heat shock proteins and proteasome activity in soleus muscles of Fisher 344 rats. Exp Gerontol. 2005; 40:37–42. [PubMed: 15664730]

Sharma AK, Bajada S, Thomas PK. Age changes in the tibial and plantar nerves of the rat. J Anat. 1980; 130:417–428. [PubMed: 7400044]

Sherman MY, Goldberg AL. Cellular defenses against unfolded proteins: a cell biologist thinks about neurodegenerative diseases. Neuron. 2001; 29:15–32. [PubMed: 11182078]

Sitte N, Merker K, Von Zglinicki T, Davies KJ, Grune T. Protein oxidation and degradation during cellular senescence of human BJ fibroblasts: part II–aging of nondividing cells. Faseb J. 2000; 14:2503–2510. [PubMed: 11099468]

Squier TC. Oxidative stress and protein aggregation during biological aging. Exp Gerontol. 2001; 36:1539–1550. [PubMed: 11525876]

Stadtman ER. Protein oxidation in aging and age-related diseases. Ann N Y Acad Sci. 2001; 928:22–38. [PubMed: 11795513]

Toth C, Shim SY, Wang J, Jiang Y, Neumayer G, Belzil C, Liu WQ, Martinez J, Zochodne D, Nguyen MD. Ndel1 promotes axon regeneration via intermediate filaments. PLoS ONE. 2008; 3:e2014. [PubMed: 18431495]

Uchida A, Brown A. Arrival, reversal, and departure of neurofilaments at the tips of growing axons. Mol Biol Cell. 2004; 15:4215–4225. [PubMed: 15215317]

Uchida A, Tashiro T, Komiya Y, Yorifuji H, Kishimoto T, Hisanaga S. Morphological and biochemical changes of neurofilaments in aged rat sciatic nerve axons. J Neurochem. 2004; 88:735–745. [PubMed: 14720223]

Vabnick I, Messing A, Chiu SY, Levinson SR, Schachner M, Roder J, Li C, Novakovic S, Shrager P. Sodium channel distribution in axons of hypomyelinated and MAG null mutant mice. J Neurosci Res. 1997; 50:321–336. [PubMed: 9373041]

Verdu E, Ceballos D, Vilches JJ, Navarro X. Influence of aging on peripheral nerve function and regeneration. J Peripher Nerv Syst. 2000; 5:191–208. [PubMed: 11151980]

Voellmy R, Boellmann F. Chaperone regulation of the heat shock protein response. Adv Exp Med Biol. 2007; 594:89–99. [PubMed: 17205678]

Weissman L, de Souza-Pinto NC, Stevnsner T, Bohr VA. DNA repair, mitochondria, and neurodegeneration. Neuroscience. 2007; 145:1318–1329. [PubMed: 17092652]

Westenbroek RE, Noebels JL, Catterall WA. Elevated expression of type II Na+ channels in hypomyelinated axons of shiverer mouse brain. J Neurosci. 1992; 12:2259–2267. [PubMed: 1318958]

Wohlgemuth SE, Julian D, Akin DE, Fried J, Toscano K, Leeuwenburgh C, Dunn WA Jr. Autophagy in the heart and liver during normal aging and calorie restriction. Rejuvenation Res. 2007; 10:281–292. [PubMed: 17665967]

Xu J, Knutson MD, Carter CS, Leeuwenburgh C. Iron accumulation with age, oxidative stress and functional decline. PLoS ONE. 2008; 3:e2865. [PubMed: 18682742]

Zanazzi G, Einheber S, Westreich R, Hannocks MJ, Bedell-Hogan D, Marchionni MA, Salzer JL. Glial growth factor/neuregulin inhibits Schwann cell myelination and induces demyelination. J Cell Biol. 2001; 152:1289–1299. [PubMed: 11257128]

Zwerling SJ, Cohen SA, Barchi RL. Analysis of protease-sensitive regions in the skeletal muscle sodium channel in vitro and implications for channel tertiary structure. J Biol Chem. 1991; 266:4574–4580. [PubMed: 1847924]

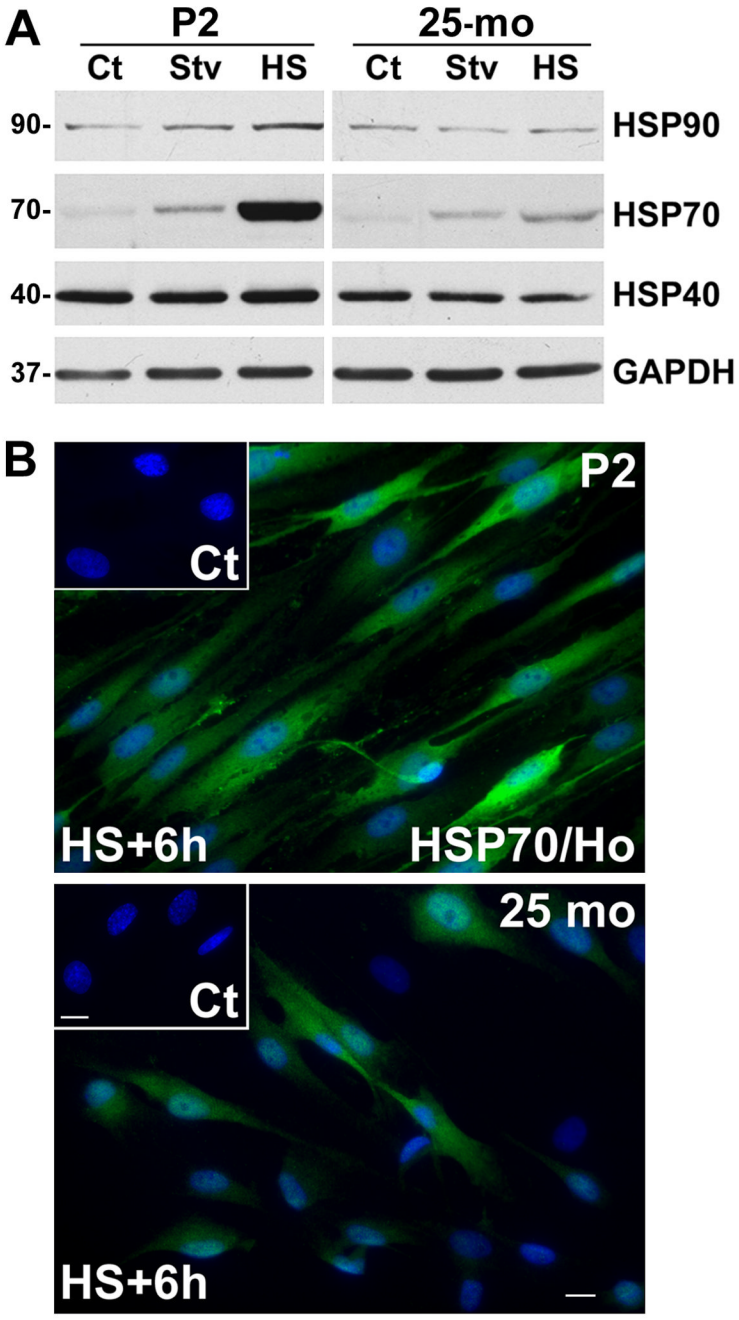

Figure 1. The chaperone response of Schwann cells from aged rats

(A) Schwann cells isolated from P2 and 25-mo rats were treated with amino acid and serum-deficient starvation (Stv) medium, or subjected to HS and allowed to recover at 37 °C for 6 h. Steady-state expression of HSP90, HSP70 and HSP40 were analyzed in whole cell lysates (15 μg/lane) of untreated control (Ct), Stv- or HS-treated samples. Blots were reprobed with anti-GAPDH antibody as a protein loading control. Molecular mass at the left, in kDa. (B) Schwann cells isolated from P2 and 25-mo old rats were subjected to HS (45 °C; 20 min) and allowed to recover at 37 °C for 6 h (HS+6h). Control untreated cells (Ct) and HS+6h samples were immunolabeled with anti-HSP70 (green) antibody. Hoechst dye (blue) was used to visualize nuclei. Scale bar, 10 μm.

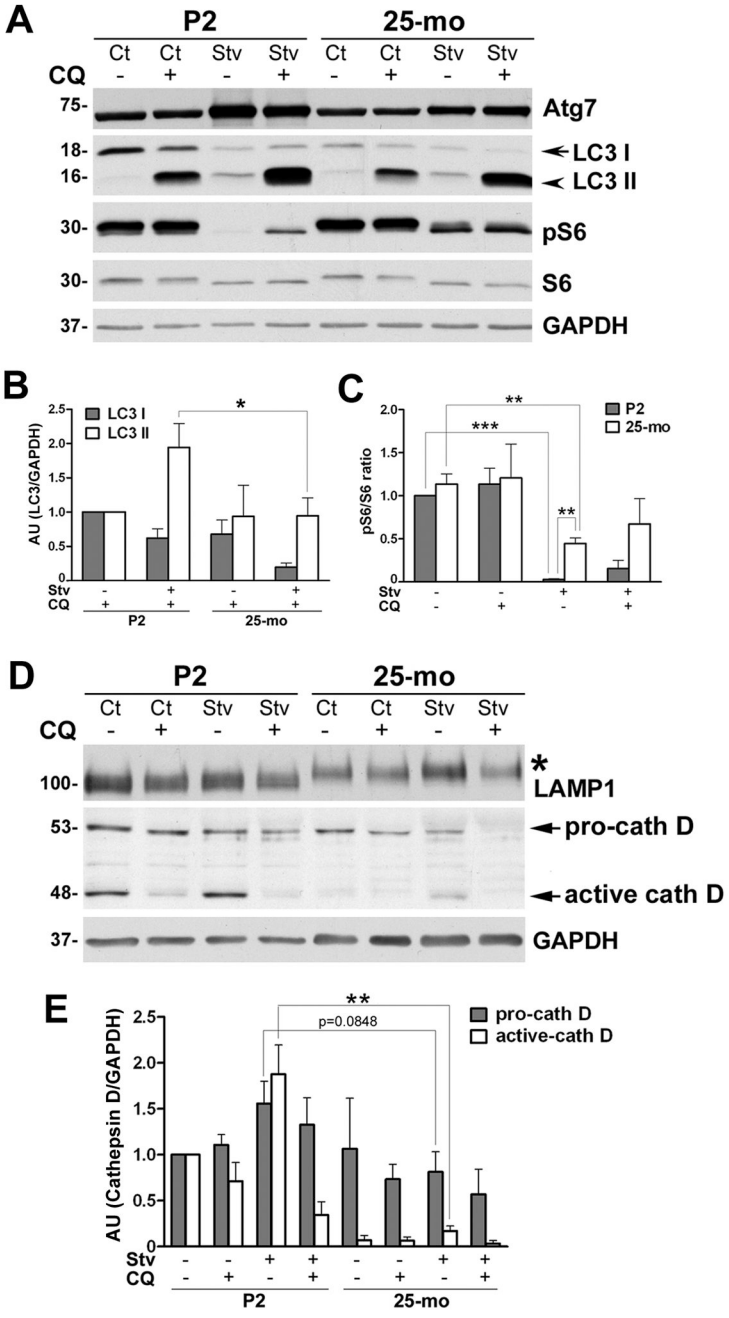

Figure 2. The response of glial cells to Stv stimulus

(A) Primary rat Schwann cells from postnatal day 2 (P2) and 25-mo old rats were maintained in normal (Control, Ct), or amino acid and serum-deficient Stv medium for 4 h, with (+) or without (−) chloroquine (CQ). The levels of autophagy markers, Atg7, LC3 I and II, pS6 and S6 were determined by Western blots (15 μg/lane). (B) Quantification of LC3 I and LC3 II band intensities in the presence of CQ normalized to GAPDH from three independent experiments are shown. LC3 I and II values of P2 cells treated with CQ was set as 1. AU:arbitrary units. (*$p<0.05$, unpaired t-test, mean ± SEM, n=3). (C) Levels of pS6 and S6 from three independent experiments were quantified and the values are represented as ratio of pS6/S6. The value of P2 Ct sample was set as 1. (D) The expression of lysosome-

associated membrane protein 1 (LAMP1) and cathepsin D were determined by Western blots. The shift in LAMP1 mobility in 25-mo samples is indicated by an asterisk. The bands representing pro-cathepsin D (pro-cath D) and active form of cathepsin D (active cath D) are marked with arrows. (E) Semi-quantitative analysis of pro-cath D and active-cath D protein levels after normalization to GAPDH from three independent experiments. The values of pro- and active-cath D in P2 Ct sample were set as 1. AU:arbitrary units. (**$p<0.01$, ***$p<0.001$, unpaired t-test, mean ± SEM). (A and D) GAPDH is shown as a protein loading control. Molecular mass at left, in kDa.

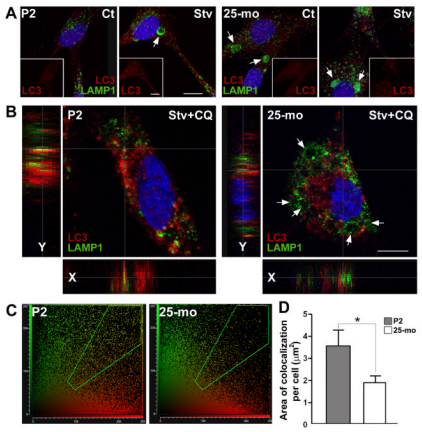

Figure 3. The fusion of autophagosomes with lysosomes in Schwann cells

(A) Composite confocal images of control (Ct) and Stv-treated (Stv) Schwann cells from postnatal day 2 (P2) and 25-mo old rats, double immunostained with anti-LC3 (red) and anti-LAMP1 (green) antibodies. Insets show LC3-like (red) staining alone. Enlarged lysosomes positive for LAMP1 (green) are indicated by arrows. (B) Mid z-stack images of cells after treatment with chloroquine (CQ), in Stv medium. Single x and y plane sections are shown at the left to reveal the interaction of autophagosomes (red) with lysosomes (green), in yellow. In cells from 25-mo old rats, swollen LAMP1-positive lysosomes (green) are indicated by arrows. Nuclei are visualized by Hoechst dye (blue). Scale bars, 10 μm. (C) 2D cytofluorograms for LC3 and LAMP1 colocalization in Stv+CQ treated P2 and 25-mo samples in which the interaction between the red channel (x-axis) and the green channel (y-axis) is highlighted in green in the diagonal region. (D) The area of colocalization (mask area) per cell was estimated using Leica software from P2 and 25-mo cells (n=200) treated with Stv+CQ from three independent experiments, and eight random visual fields per condition (*$p<0.05$, unpaired t-test, mean ± SEM).

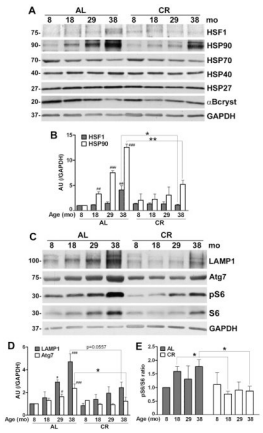

Figure 4. Age-associated alterations in chaperones and autophagic proteins in myelinated peripheral nerves

(A) Total sciatic nerve lysates (25 μg/lane) from the indicated ages and diet were analyzed with anti-heat shock factor 1 (HSF1) antibody. The same nerve lysates (20 μg/lane) were also probed with antibodies against HSP90, HSP70, HSP40, HSP27 and αB-crystallin. (B) Quantification of HSF1 and HSP90 protein levels normalized to GAPDH from three independent experiments ($^{\#\#}p<0.01$, $^{\#\#\#}p<0.001$, Fisher's PLSD, mean ± SEM), AU: arbitrary units. The effect of CR on these proteins was analyzed by comparing HSF1 or HSP90 protein values with age-matched AL counterparts (*p<0.05, **p<0.05, unpaired t-test, mean ± SEM). (C) Steady-state levels of LAMP1, Atg7, pS6 and S6 proteins in sciatic nerves from AL and CR rats were analyzed by Western blots. Blots were reprobed with anti-GAPDH antibody as protein loading control. Molecular mass at the left, in kDa. (D) Quantification of LAMP1 and Atg7 protein levels normalized to GAPDH from three independent experiments ($^{\#}p<0.05$, $^{\#\#\#}p<0.001$, Fisher's PLSD analysis, *p<0.05, unpaired t-test, mean ± SEM). (E) Blots of pS6 and S6 from three independent experiments were quantified and the values are represented as ratio of pS6/S6. The pS6/S6 ratio of 8-mo old AL sample was set as 1 (*p<0.05, unpaired t-test, mean ± SEM). A-D, n=3 rats per condition.

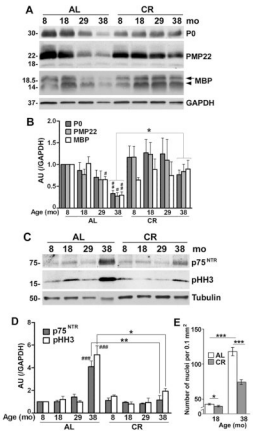

Figure 5. CR preserves myelin protein expression and myelinating Schwann cell phenotype

(A) Total sciatic nerve lysates (10 μg/lane) from AL and CR rats at 8, 18, 29 and 38-mo ages were analyzed with antibodies against protein zero (P0), peripheral myelin protein 22 (PMP22) and myelin basic protein (MBP) by Western blots. The arrow and arrowhead on the right indicate the 18.5 and 14 kDa of isoforms of MBP. GAPDH serves as a protein loading control. (B) Densitometric analysis of myelin proteins P0, PMP22 and MBP normalized to GAPDH ($^{\#}p<0.05$, $^{\#\#}p<0.01$ [Fisher's PLSD], *p<0.05 [unpaired t-test], mean ± SEM). (C) Total sciatic nerve lysates (20 μg/lane) from rats under AL and CR diet were analyzed by Western blotting with polyclonal anti-$p75^{NTR}$ and monoclonal anti-pHH3 antibodies. The blots were reprobed with anti-tubulin to monitor protein loading. Molecular mass at left, in kDa. (D) Quantification of $p75^{NTR}$ and pHH3 normalized to GAPDH ($^{\#\#\#}p<0.001$ [Fisher's PLSD], *p<0.05, *p<0.01, ***p<0.001 [unpaired t-test]). (E) The nuclei of Schwann cells were counted in longitudinal sections of sciatic nerves from two different depths and eight random visual fields ($0.1mm^2$) per animal. (*p<0.05, ***p<0.001, unpaired t-test, mean ± SEM). A-E, n=3 rats per condition.

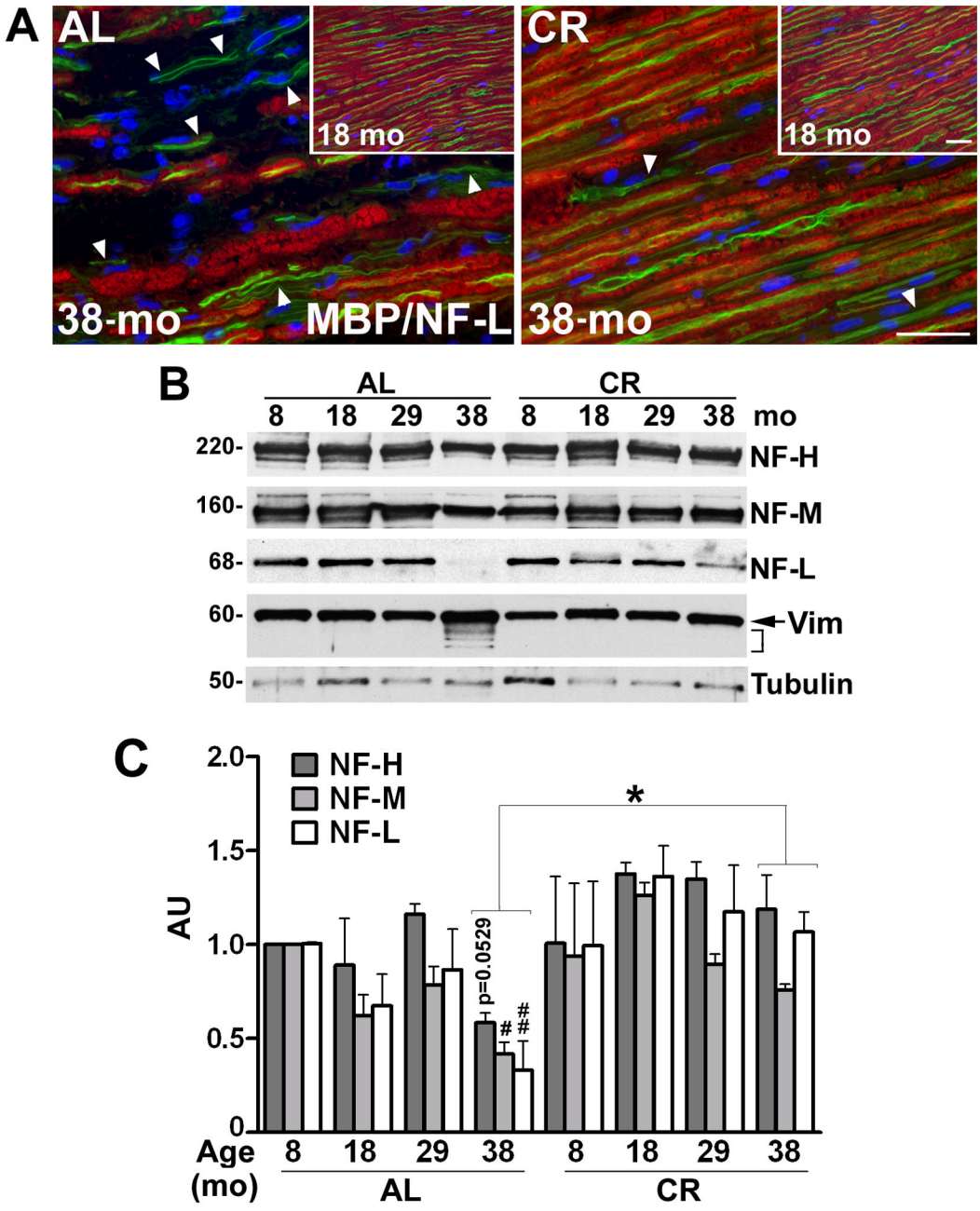

Figure 6. The expression of axonal proteins is supported by CR diet

(A) The severe reduction in MBP-like (red) as well as NF-L-like (green) staining is shown on longitudinal sections of sciatic nerves of 38-mo old AL-fed rats. Arrowheads indicate nerve fibers positive for neurofilaments but devoid of MBP-reactive myelin. Nerves from 18-mo old AL and CR rats are shown in the insets on the right. Nuclei are stained with Hoechst dye (blue). Scale bars, 40 μm. (B) Total sciatic nerve lysates (10 μg/lane) of AL and CR rats from the indicated ages were analyzed with antibodies against neurofilament proteins, NF-H, NF-M, NF-L and the intermediate filament protein, vimentin. The arrow indicates the full-length form (60 kDa) and the bracket shows the proteolytic cleavage products of vimentin. Tubulin serves as a protein loading control. Molecular mass at left, in

kDa. (C) Densitometric analysis of neurofilament proteins NF-H, -M and -L normalized to tubulin from three independent sets of blots ($^{\#}p<0.05$, $^{\#\#}p<0.01$ (Fisher's PLSD), $^{*}p<0.05$ (unpaired t-test), mean ± SEM, n=3 rats). AU:arbitrary units.

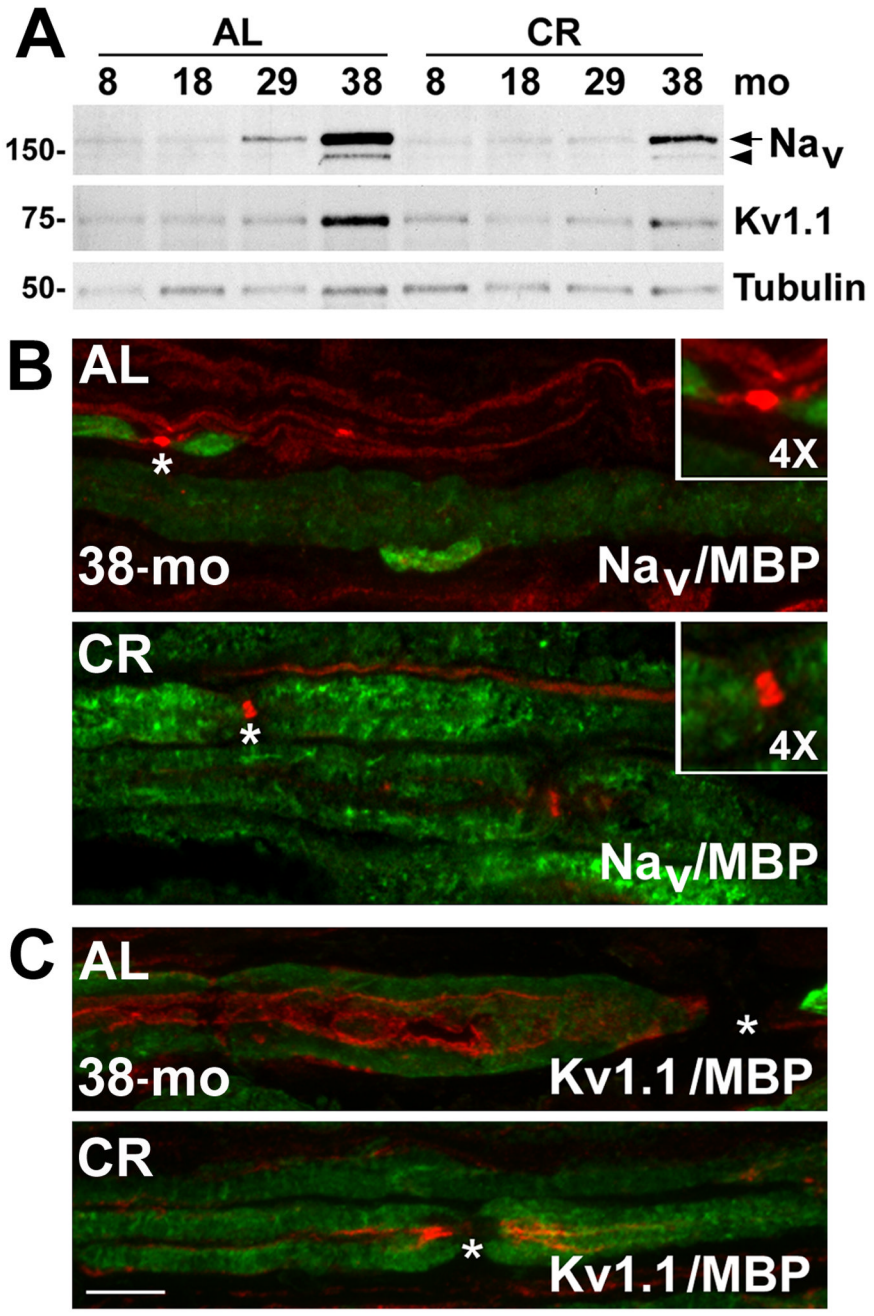

Figure 7. The expression and localization of Na^+ and K^+ channel proteins in myelinated nerves of aged rats

(A) Lysates of sciatic nerves (25 μg/lane) from the indicated ages and diet regimen (AL and CR) were assayed by Western blots for the expression of pan-voltage gated sodium channels (Na_v) and a subtype of voltage gated potassium channel (Kv1.1) with polyclonal anti-pan Na_v and anti-Kv1.1 antibodies, respectively. The arrow indicates the full length α-subunit of Na_v and the arrowhead points to its proteolytic cleavage product. Tubulin serves as a protein loading control. Molecular mass at left, in kDa. (B) Longitudinal sciatic nerve sections were co-immunolabeled with anti-pan Na_v (red) and anti-MBP (green) antibodies (panel on right). The node of Ranvier, as marked by clustered Na_v channel-like staining (asterisk) is enlarged

4× in the inset. (C) Localization of Kv1.1 channel was visualized in longitudinal sciatic nerve sections from 38-mo old AL and CR rats by co-immunolabeling with anti-Kv1.1 (red) and anti-MBP (green) antibodies (panel on right). The nodes of Ranvier are marked by asterisks. Scale bar, 10 μm.

Table 1

Primary antibodies used in this study

Species	Antigen	Source and Catalog #	Dilution	
			WB	IS
Chicken	P0	Gift from Dr.Gerry Shaw, UF	1:10000	1:500
Rabbit	PMP22	Pareek et. al, 1997; n/a	1:1000	n/a
Rat	MBP	Chemicon, Temecula; MAB386	1:5000	n/a
Mouse	GAPDH	Encor Biotechnology Inc.; MCA-1D4	1:5000	n/a
Mouse	NF-H	Encor Biotechnology Inc.; MCA-NAP4	1:500	n/a
Chicken	NF-M	Encor Biotechnology Inc.; CPCA-NF-M	1:5000	n/a
Chicken	NF-L	Encor Biotechnology Inc.; CPCA-NF-L	1:5000	1:1000
Mouse	Vimentin	Sigma, St Louis, MO, USA; clone VIM 13.2	1:1000	1:500
Chicken	MBP	Encor Biotechnology, Inc.; CPCA-MBP	n/a	1:500
Rabbit	$p75^{NTR}$	Chemicon; AB1554	1:10000	n/a
Mouse	pHH3 (Ser10)	Millipore, Temecula; 05–598	1:500	1:200
Rabbit	Pan-Na_v (α-subunit)	Chemicon; AB5210	1:250	1:100
Rabbit	Kv1.1	Chemicon; AB5174	1:250	1:100
Rabbit	HSF1	Stressgen; Victoria British Columbia; SPA-901	1:500	1:250
Rat	HSP90	Stressgen, SPA-835	1:2000	n/a
Rabbit	HSP70	Stressgen; SPA-812	1:1000	1:500
Rabbit	HSP40	Stressgen; SPA-400	1:2000	n/a
Goat	HSP27	Santa Cruz Biotechnology, Inc.; sc-1049	1:2000	n/a
Rabbit	αB-crystallin	Stressgen; SPA-223	1:1000	n/a
Rabbit	LAMP1	Gift from Dr. William Dunn Jr, UF	1:2000	n/a
Rabbit	Atg7	Gift from Dr. William Dunn Jr, UF	1:3000	n/a
Rabbit	pS6 (Ser235/236)	Cell Signaling Technology, Inc., 2211	1:800	n/a
Mouse	S6	Cell Signaling Technology, Inc.; 2317	1:800	n/a
Mouse	HSP70	Stressgen; SPA-810	1:1000	1:250
Mouse	LAMP1	Stressgen; VAM-EN001	n/a	1:250
Rabbit	Cathepsin-D	Cortex Biochem, San Leanardo, CA, USA; CP3090	1:1000	n/a
Rabbit	LC3	Cell Signaling Technology; 2775	1:1000	1:200

WB: Western Blot; IS: Immunostaining; n/a: non-applicable